

Equilibrium First-Order Melting and Second-Order Glass Transitions of the Vortex Matter in $\text{Bi}_2\text{Sr}_2\text{CaCu}_2\text{O}_8$

H. Beidenkopf,^{1,*} N. Avraham,¹ Y. Myasoedov,¹ H. Shtrikman,¹ E. Zeldov,¹
B. Rosenstein,^{1,2} E.H. Brandt,³ and T. Tamegai⁴

¹*Department of Condensed Matter Physics, Weizmann Institute of Science, Rehovot 76100, Israel*

²*National Center for Theoretical Sciences and Electrophysics Department,
National Chiao Tung University, Hsinchu 30050, Taiwan, R.O.C.*

³*Max-Planck-Institut für Metallforschung, Heisenbergstr. 3, D-70506 Stuttgart, Germany*

⁴*Department of Applied Physics, The University of Tokyo, Hongo, Bunkyo-ku, Tokyo 113-8656, Japan
(Dated: June 26, 2018)*

The thermodynamic $H - T$ phase diagram of $\text{Bi}_2\text{Sr}_2\text{CaCu}_2\text{O}_8$ was mapped by measuring local *equilibrium* magnetization $M(H, T)$ in presence of vortex ‘shaking’. Two equally sharp first-order magnetization steps are revealed in a single temperature sweep, manifesting a liquid-solid-liquid sequence. In addition, a second-order glass transition line is revealed by a sharp break in the equilibrium $M(T)$ slope. The first- and second-order lines intersect at intermediate temperatures, suggesting the existence of four phases: Bragg glass and vortex crystal at low fields, glass and liquid at higher fields.

PACS numbers: 74.25.Qt, 74.25.Dw, 74.72.Hs, 64.70.Pf

The magnetic field vs. temperature ($H - T$) phase diagram of the vortex matter in high-temperature superconductors, and in $\text{Bi}_2\text{Sr}_2\text{CaCu}_2\text{O}_8$ (BSCCO) *in particular*, has drawn extensive scientific attention [1]. The commonly cited thermodynamic phase diagram of BSCCO currently consists of a single unified first-order (FO) melting line. It separates the low-field quasi long-range ordered Bragg glass (BrG) phase from the high-field liquid and glass phases [1, 2, 3, 4, 5, 6]. It is not clear, however, whether the two high-field disordered phases are thermodynamically distinct, or rather reflect a gradual dynamic cross-over *from liquid into a frozen, pinned state upon cooling* [7, 8]. In this letter we show that the equilibrium phase diagram of the vortex matter is indeed more diverse than the one usually considered.

Experimentally, one of the main obstacles in mapping the low-temperature thermodynamics of the vortex matter is its logarithmically slow relaxation rate. Consequently, the phase diagram has been studied in the past mostly through dynamic phenomena. Two prime examples are the irreversibility line itself, *marking* the onset of hysteresis, and the second magnetization peak (SMP), observed along such hysteretic magnetization loops [9].

Recently, though, vortex ‘shaking’ was shown to be extremely effective in catalyzing relaxation at low temperatures [2, 10, 11]. Its application unveiled the inverse melting and the thermodynamic FO transition as the phenomenon underlying the non-equilibrium SMP [2]. The ‘shaking’ method employs the segregated penetration of an in-plane field component into the highly anisotropic BSCCO samples in the form of Josephson vortices, which are confined in between the CuO_2 planes. In the presence of an *ac* in-plane field, the Josephson vortices instantaneously bisect the pancake vortex (PV) stacks on their passage, interacting mainly with adjacent

PVs, while most of the PVs in the stack remain at rest [12]. These occasional interactions agitate pinned PVs, assisting them in assuming their equilibrium configuration.

Within the present study we performed local magnetization measurements by field and temperature sweeps, while utilizing the ‘shaking’ method, to map the *equilibrium* phase diagram of the vortex matter. The cross-mapping of the FO melting line along both sweeping directions *shows an excellent agreement*. Temperature sweeps provided particularly sharp features, with which we demonstrate a liquid-solid-liquid sequence of phases. Ertaş and Nelson [13] have predicted such a liquid-solid-liquid sequence to occur within a single temperature sweep, but it was never observed experimentally. We further find evidence of a *novel second order (SO) phase transition* within the vortex solid phase, which bears important consequences regarding the nature of the BrG phase.

The reported results were obtained with a slightly over-doped BSCCO crystal with $T_c \approx 90$ K grown by the travelling solvent floating zone method [14]. This specific sample was polished into a triangular prism of base $660 \times 270 \mu\text{m}^2$ and height $70 \mu\text{m}$ [15] (other samples yielded similar results, to be presented elsewhere). The sample was attached onto an array of eleven $10 \times 10 \mu\text{m}^2$ GaAs/AlGaAs Hall sensors. In all measurements taken below 60 K the sample was subject to a 10 Hz in-plane *ac* field of amplitude 350 Oe, which was aligned parallel to the planes to an accuracy of a few millidegrees. Note that according to the anisotropic scaling theory [1] this in-plane field is effectively attenuated by a factor $\gamma \simeq 200$ - the anisotropy constant in BSCCO. We found that at higher temperatures ‘shaking’ had no effect on the FO transition besides a small broadening (see below).

The field sweep mapping of the FO melting line is shown in Fig. 1. The collapse of the hysteretic magnetization into a reversible behavior upon ‘shaking’ is demonstrated in Fig. 1a taken at 32 K. A reversible magnetization step appears instead of the SMP. To better resolve the step we plot in Fig. 1b the derivative of the measured induction with respect to applied field dB/dH . The FO transition thus appears reversibly as a δ -like peak (red) on top of the $dB/dH \approx 1$ (blue) background. Figure 1c shows a color scheme of the derivatives dB/dH measured by field sweeps within the temperature range 28–80 K. The individual melting peaks combine to give the locus of the FO transition line $H_m(T)$. Its negative slope at elevated temperatures becomes positive below 38 K. This non-monotonic behavior marks the change in the character of the transition from thermally-induced above the extremum to disorder-driven in the inverse melting region [5, 6, 13].

In addition to the field sweeps, our experimental setup also enables temperature sweeps in the presence of vortex ‘shaking’. It thus allows to measure directly the temperature dependence of the equilibrium magnetization at a constant applied c-axis field. At fields slightly lower than 390 Oe (e.g. at 380 Oe along the dashed line in Fig. 2a) these sweeps should cross the melting line twice. Remarkably, the measured local induction in Fig. 2b indeed shows two very clear and opposite equilibrium magnetization steps on both descending and ascending sweeps. Note that for clarity we have subtracted from the data a

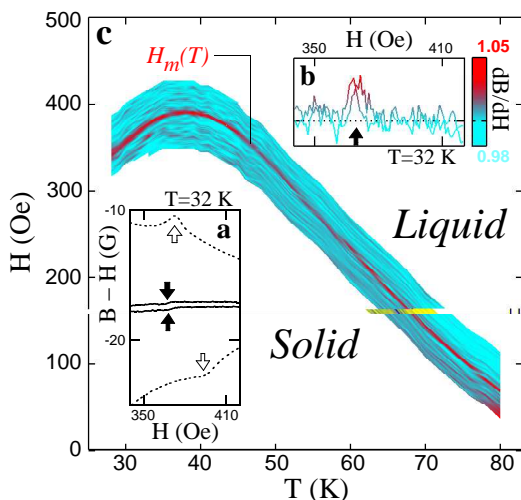


FIG. 1: (color online) (a) 32 K field sweeps with (solid) and without (dotted) an in-plane 350 Oe-10 Hz ‘shaking’ field. Reversible steps in magnetization (solid arrows) appear instead of the hysteretic SMP (open arrows) upon shaking. (b) The derivative of the induction with respect to applied field dB/dH at 32 K as a color scheme. The first-order transition appears as a paramagnetic peak (red) on top of the $dB/dH \approx 1$ background (blue). (c) Successive mapping of the first-order melting line $H_m(T)$ measured by field sweeps.

linear slope αT . It is contributed both by the slight temperature dependence of the Hall coefficients of the sensors and by the linear term of the magnitude of the diamagnetic equilibrium magnetization, which monotonically decreases with temperature. This is the first observation of two FO transitions obtained in a single temperature sweep. Moreover, the two steps are equally sharp and with comparable heights of about 0.15 G. This demonstrates that the thermally- and disorder-driven processes, responsible for the melting and the inverse melting respectively, are equivalent mechanisms leading to a FO destruction of the quasi-ordered vortex solid.

The temperatures at which the magnetization steps appear along the temperature sweep of Fig. 2b are in complete agreement with the melting behavior deduced from field sweeps (dotted lines). Therefore, the *transition line* in Fig. 2a is independent of the specific $H - T$ path along which it is approached - a mandatory equilibrium property. The remaining small hysteresis of 0.1 to 0.2 G between downward and upward sweeps apparently results from surface barrier effects, while the vortices in the bulk are well equilibrated by the ‘shaking’. The finite widths (about 0.7 K) that the melting steps attain are mainly due to a spatial and a temporal averaging mechanisms. The first is introduced by the sensor’s finite active area that averages over the propagating melting front [16], which results from the spatially inhomogeneous equilibrium magnetization profile [17]. The temporal one is a

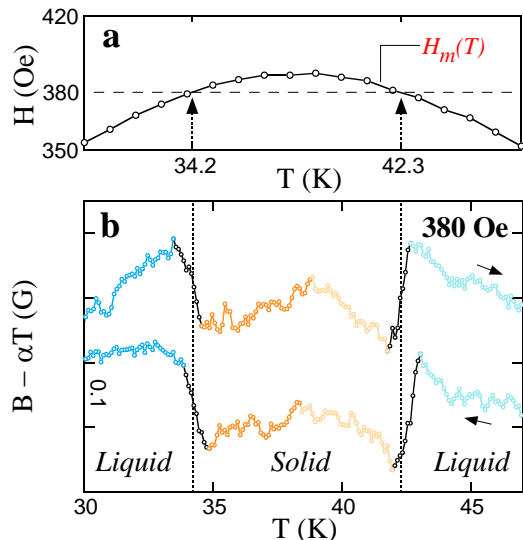


FIG. 2: (color online) (a) The FO melting line $H_m(T)$ mapped via field sweeps (open circles). (b) Local induction $B(T)$ in the presence of ‘shaking’, measured upon temperature sweep at 380 Oe along the dashed line in (a). A linear slope αT was subtracted for clarity. The two equally narrow FO magnetization steps (black segments) show a liquid-solid-liquid sequence. The temperatures at which the phase transitions occur coincide with those, extracted from field sweeps (dotted lines). The color code reflects different phases in Fig. 4.

by-product of the ‘shaking’ technique. The in-plane field component is known to slightly reduce the melting temperature [12, 18, 19]. Consequently, our time averaged measurement in the presence of the *ac* in-plane ‘shaking’ field results in an additional broadening due to the instantaneous periodic shift of the effective local melting temperature.

We thus turn to report the detection of a novel phase transition, whose signature is a distinct break in the slope of the magnetization $M(T)$. It is visible around 37 K in Fig. 2b at 380 Oe, and becomes much more pronounced at fields further away from the extremum of the FO melting line, as depicted by Fig. 3. The 420 Oe temperature sweep (Fig. 3a) does not intersect with the FO line, hence no steps appear in the local induction. Nevertheless, a sharp break in slope is clearly resolved along both descending and ascending temperature sweeps at T_g . A sharp reversible break in the induction slope appears also in the 350 Oe temperature sweep of Fig. 3b (dotted line) in between the two melting steps, hence within the solid phase. This non-analytic behavior is emphasized by the sharp step in the derivative dB/dT shown in the insets. *These kinks were found also in other samples and at various Hall-sensor locations, and did not depend on the sweeping rate.* We thus conclude, that this break in slope of the *equilibrium magnetization* $M(T)$ indicates a thermodynamic SO phase transition.

Mapping of both the first-order $H_m(T)$ and second-order $H_g(T)$ transition lines onto the equilibrium $H - T$ phase diagram is given in Fig. 4. The SO line (solid dots) intersects the melting curve (open circles), and shows weak field dependence throughout the mapped region (and therefore cannot be readily observed by field sweeps). The resulting phase diagram consists of *four* distinct thermodynamic phases.

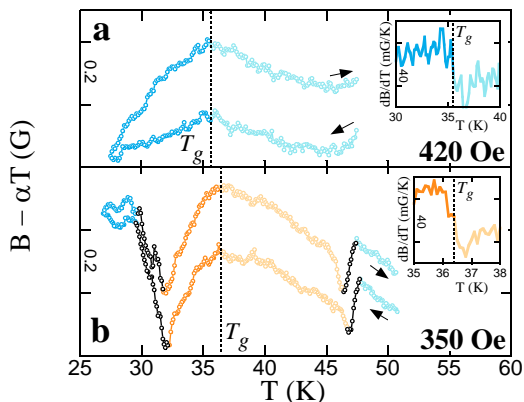


FIG. 3: (color online) Local induction $B(T)$, measured along temperature sweeps while ‘shaking’. A reversible sharp break in the slope (at the dotted lines) appears both above (a - 420 Oe) and below (b - 350 Oe) the melting line $H_m(T)$. The insets show a corresponding step in the derivative dB/dT , signifying a thermodynamic second-order phase transition.

The high-field part of the novel SO line can be naturally identified with the long sought glass transition line. It asserts that the low-temperature glass phase is indeed thermodynamically distinct from the high-temperature liquid one. Several experimental studies have observed bulk irreversibility features in BSCCO, which appeared above $H_m(T)$ at about 35 K [20, 21]. However, all these studies probed dynamic or non-equilibrium vortex properties. The glass line of Fig. 4 is the first experimental evidence of such a thermodynamic transition in BSCCO.

Yet, the most intriguing result in Fig. 4 is the detection of the SO line within the vortex solid region (orange). This implies that two distinct thermodynamic phases are present in the low-field region below $H_m(T)$, contrary to the common belief that a single BrG phase prevails throughout this part of the phase diagram. A number of previous studies indicated a depinning line of similar topology within the BrG below $H_m(T)$ [20]. However, all these measurements probed only the non-equilibrium properties, which were consistent with the existing theoretical dynamic predictions and simulations of depinning [13, 22]. In contrast, the present finding of a thermodynamic line requires a more fundamental reconsideration.

It is interesting to note that in $\text{YBa}_2\text{Cu}_3\text{O}_7$ crystals a thermodynamic signature of a SO transition within the liquid phase has been reported [23]. There, however, the SO line emanates from the upper critical point of the FO line, directly extending it to higher fields. This topology is consistent with several dynamic measurements in $\text{YBa}_2\text{Cu}_3\text{O}_7$ [24, 25], although alternative topologies have been also suggested [26, 27]. In contrast, our thermodynamic data of BSCCO show that the SO

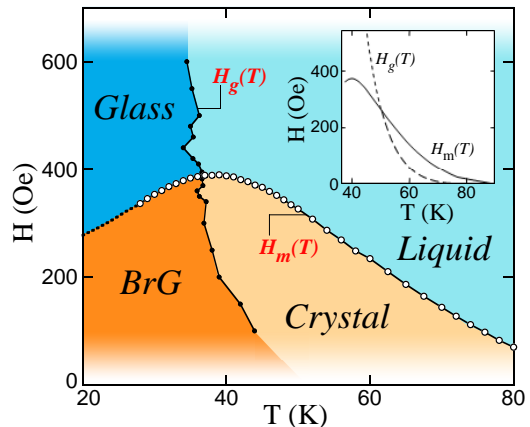


FIG. 4: (color online) The thermodynamic phase diagram of BSCCO accommodates *four* distinct phases, separated by a first-order melting line $H_m(T)$ (open circles), which is intersected by the second-order glass line $H_g(T)$ (solid dots). The inset plots an equivalent phase diagram, calculated based on Ref. 31, consisting of a second-order replica symmetry breaking lines $H_g(T)$ both above (dotted) and below (dashed) the first-order transition $H_m(T)$ (solid).

and the FO transitions are two independent lines that intersect each other nearly at a right angle.

Several theoretical studies have shown that under the elastic medium approximation quasi long-range order of the vortex lattice is still retained in the presence of quenched disorder, giving rise to the BrG phase [28, 29]. This phase was found to be stable at all temperatures (as long as topological excitations are excluded) in systems of dimensionality greater than two and lower than four. This is probably the reason why a non-topological thermodynamic phase transition of the BrG phase was hardly ever considered in 3D models. An exception is a Josephson-glass line that was suggested to exist within the BrG region [30]. Still, the general belief is that the BrG phase is robust until dislocations proliferate, which gives rise to the FO phase transition [6, 8, 28]. In 2D systems, however, the BrG models did find a possible finite-temperature depinning transition, above which disorder is no longer relevant. Therefore, the observed SO transition could be accounted for within these models only in the extreme case of vanishing coupling between the superconducting layers.

In contrast, in a recent theoretical work [31] the free energy of the vortex matter in the presence of quenched disorder was explicitly calculated under the lowest-Landau-level approximation in a 3D model. It was found that two transitions are present: a FO melting, at which the quasi long-range order is destroyed, and a SO glass transition, below which the replica symmetry is spontaneously broken. The inset of Fig. 4 shows the phase diagram, calculated using a similar effective 2D model with parameters optimized for BSCCO [32]. The calculations reproduce the measured features very well. Amongst them are the melting and inverse-melting behavior, the discontinuity of the magnetization slope dM/dT at the glass transition, and the $H_g(T)$ line itself, which resides at slightly higher temperatures as compared to experiment. In addition, the calculations show that the portions of the $H_g(T)$ line, lying above and below the FO transition $H_m(T)$ (dotted and dashed lines, respectively), are slightly shifted from each other. Therefore, they do not cross the melting line at a single point, but rather form two closely located tricritical points along it. This minute shift can hardly be seen in the inset of Fig. 4, and is below our current experimental resolution.

Within this model the high-field glass phase and the low-field BrG are strongly pinned and replica symmetry broken, whereas the two high-temperature phases are replica symmetric and thus reversible. This conclusion of reversibility is consistent also with the existing dynamic measurements [20]. It is therefore tempting to speculate that the phase above $H_g(T)$ and below $H_m(T)$ should acquire a true crystalline order. However, since Rosenstein and Li did not calculate the structure factor and our measurements do not probe this quantity, the proposed vortex crystal phase certainly calls for further experimen-

tal and theoretical investigations.

In summary, we present thermodynamic evidence of a possibly second-order glass transition line that splits the quasi-ordered vortex solid into two distinct phases. By comparing the results with existing dynamic measurements and a new theoretical study, we suggest that the two phases are BrG and a vortex crystal. The glass line crosses the first-order melting line near its extremum and extends to higher fields, giving rise to two thermodynamically distinct disordered phases - a glass and a liquid.

We thank D. Li, V.M. Vinokur, and B. Horovitz for stimulating discussions. This work was supported by the Israel Science Foundation Center of Excellence, by the German-Israeli Foundation G.I.F., by the Minerva Foundation, Germany, and by Grant-in-aid for Scientific Research from the Ministry of Education, Culture, Sports, Science, and Technology, Japan. BR acknowledges the support of the Albert Einstein Minerva Center for Theoretical Physics and EZ the US-Israel Binational Science Foundation (BSF).

* Electronic address: haim.beidenkopf@weizmann.ac.il

- [1] G. Blatter and V.B. Geshkenbein, *The Physics of Superconductors* (Springer, 2003), vol. I, chap. 10, p. 725.
- [2] N. Avraham *et al.*, *Nature* **411**, 451 (2001).
- [3] Y. Radzyner, A. Shaulov, and Y. Yeshurun, *Phys. Rev. B* **65**, 100513(R) (2002).
- [4] V. Vinokur *et al.*, *Physica C* **295**, 209 (1998).
- [5] G.P. Mikitik and E.H. Brandt, *Phys. Rev. B* **68**, 054509 (2003); J. Kierfeld and V. Vinokur, *Phys. Rev. B* **69**, 24501 (2004).
- [6] T. Giamarchi and S. Bhattacharya, *High Magnetic Fields: Applications in Condensed Matter Physics, Spectroscopy* (Springer, 2002), p. 314.
- [7] C. Reichhardt, A. van Otterlo, and G.T. Zimányi, *Phys. Rev. Lett.* **84**, 1994 (2000).
- [8] Y. Nonomura and X. Hu, *Phys. Rev. Lett.* **86**, 5140 (2001); P. Olsson and S. Teitel, *Phys. Rev. Lett.* **87**, 137001 (2001).
- [9] B. Khaykovich *et al.*, *Phys. Rev. Lett.* **76**, 2555 (1996).
- [10] M. Willemin *et al.*, *Phys. Rev. Lett.* **81**, 4236 (1998).
- [11] G.P. Mikitik and E.H. Brandt, *Phys. Rev. B* **69**, 134521 (2004).
- [12] A.E. Koshelev, *Phys. Rev. Lett.* **83**, 187 (1999).
- [13] D. Ertas and D.R. Nelson, *Physica C* **272**, 79 (1996).
- [14] N. Motohira *et al.*, *J. Ceram. Soc. Jpn. Int.* **97**, 994 (1989).
- [15] D. Majer, E. Zeldov, and M. Konczykowski, *Phys. Rev. Lett.* **75**, 1166 (1995).
- [16] A. Soibel *et al.*, *Nature* **406**, 282 (2000).
- [17] E. Zeldov *et al.*, *Phys. Rev. Lett.* **73**, 1428 (1994).
- [18] S. Ooi *et al.*, *Phys. Rev. Lett.* **82**, 4308 (1999).
- [19] B. Schmidt *et al.*, *Phys. Rev. B* **55**, R8705 (1997).
- [20] D.T. Fuchs *et al.*, *Phys. Rev. Lett.* **80**, 4971 (1998); C.D. Dewhurst and R.A. Doyle, *Phys. Rev. B* **56**, 10832 (1997); Y. Yamaguchi *et al.*, *Phys. Rev. B* **63**, 014504 (2000); S. Ooi, T. Mochiku, and K. Hirata, *Physica C* **378**, 523 (2002); Y. Matsuda *et al.*, *Phys. Rev. Lett.*

- 78**, 1972 (1997); S. Ooi, T. Shibaushi, and T. Tamegai, Physica B **284**, 775 (2000).
- [21] T. Shibauchi *et al.*, Phys. Rev. Lett. **83**, 1010 (1999).
- [22] R. Sugano *et al.*, Physica C **357**, 428 (2001).
- [23] F. Bouquet *et al.*, Nature **411**, 448 (2001).
- [24] H. Safar *et al.*, Phys. Rev. Lett. **70**, 3800 (1993).
- [25] W.K. Kwok *et al.*, Phys. Rev. Lett. **84**, 3706 (2000).
- [26] K. Shibata *et al.*, Phys. Rev. B **66**, 214518 (2002).
- [27] B.J. Taylor *et al.*, Phys. Rev. B **68**, 054523 (2003).
- [28] T. Giamarchi and P. LeDoussal, Phys. Rev. B **52**, 1242 (1995).
- [29] T. Nattermann, Phys. Rev. Lett. **64**, 2454 (1990).
- [30] B. Horovitz and T.R. Goldin, Phys. Rev. Lett. **80**, 1734 (1998); B. Horovitz, Phys. Rev. B **72**, 024519 (2005).
- [31] D. Li and B. Rosenstein, Phys. Rev. Lett. **90**, 167004 (2003); D. Li and B. Rosenstein, cond-mat/0411096.
- [32] B. Rosenstein and D. Li, unpublished.